



Published in final edited form as:

*Chem Biol Drug Des.* 2017 February ; 89(2): 192–206. doi:10.1111/cbdd.12792.

## Design features for optimization of tetrapyrrole macrocycles as antimicrobial and anticancer photosensitizers

Alejandra Martinez De Pinillos Bayona<sup>1,2</sup>, Pawel Mroz<sup>3</sup>, Connor Thunshelle<sup>1,4</sup>, and Michael R Hamblin<sup>1,5,6,\*</sup>

<sup>1</sup>Wellman Center for Photomedicine, Massachusetts General Hospital, Boston, MA 02114, USA

<sup>2</sup>Division of Surgery & Interventional Science, University College London, Royal Free Hospital, London, NW3 2PF, UK

<sup>3</sup>Dept of Pathology, University of Michigan Medical School, Ann Arbor, MI 48109, USA

<sup>4</sup>Harvard College, Cambridge, MA 02138, USA

<sup>5</sup>Department of Dermatology, Harvard Medical School, Boston, MA 02115, USA

<sup>6</sup>Harvard-MIT Division of Health Sciences and Technology, Cambridge, MA 02139, USA

### Abstract

Photodynamic therapy (PDT) uses non-toxic dyes called photosensitizers (PS) and harmless visible light that combine to form highly-toxic reactive oxygen species that kill cells. Originally a cancer therapy, PDT now includes applications for infections. The most widely studied PS are tetrapyrrole macrocycles including porphyrins, chlorins, bacteriochlorins and phthalocyanines. The present review covers the design features in PS that can work together to maximize the PDT activity for various disease targets. Photophysical and photochemical properties include the wavelength and size of the long-wavelength absorption peak (for good light penetration into tissue), the triplet quantum yield and lifetime, and the propensity to undergo Type I (electron-transfer) or Type II (energy-transfer) photochemical mechanisms. The central metal in the tetrapyrrole macrocycle has a strong influence on the PDT activity. Hydrophobicity and charge are important factors that govern interactions with various types of cells (cancer and microbial) in vitro, and the pharmacokinetics and biodistribution in vivo. Hydrophobic structures tend to be water-insoluble and require a drug delivery vehicle for maximal activity. Molecular asymmetry and amphiphilicity are also important for high activity. In vivo some structures possess the ability to selectively accumulate in tumors, and to localize in the tumor microvasculature producing vascular shutdown after illumination.

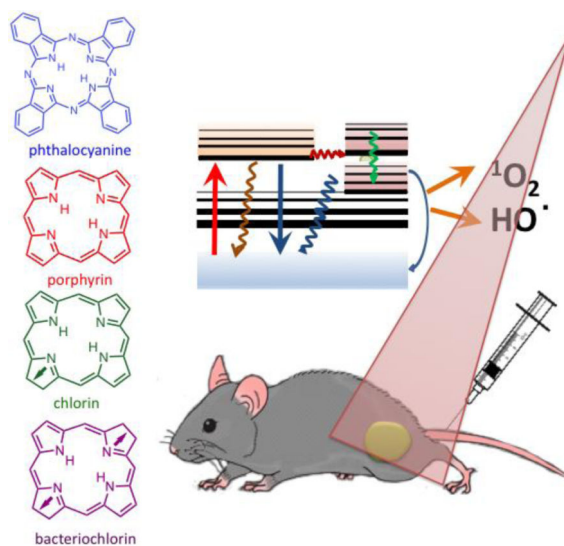
### Graphical abstract

---

\* correspondence to: 40 Blossom Street, BAR414, Boston, MA 02114; Hamblin@helix.mgh.harvard.edu; phone: 617 726 6182; fax 617 726 6643.

#### Conflict of Interest.

The authors declare no conflict of interest.



Photodynamic therapy (PDT) uses non-toxic dyes called photosensitizers (PS) and harmless visible light that combine to form highly-toxic reactive oxygen species that kill cells. PS are often tetrapyrrole macrocycles including porphyrins, chlorins, bacteriochlorins and phthalocyanines. We discuss drug-design parameters including hydrophobicity, charge, molecular asymmetry that influence subcellular localization and pharmacokinetics.

## Keywords

photodynamic therapy; photosensitizer; porphyrin; chlorin; bacteriochlorin; phthalocyanine; biuodistribution; pharmacodynamics

## 1. Photodynamic therapy

Photodynamic therapy (PDT) has been employed with moderate success in management of a variety of solid tumors and many non-malignant diseases. PDT is a two-step procedure that involves the administration of a particular dye called a photosensitizer (PS), followed by activation of the drug with nonthermal light of a specific wavelength [1–4]. Therefore, the biological responses to the activated PS are restricted to the particular areas of tissue exposed to light. PDT as a treatment procedure has been approved by the United States Food and Drug Administration for use in endobronchial and endoesophageal treatment [5, 6] and also as a treatment for premalignant and early malignant diseases of the skin (actinic keratoses), bladder, breast, stomach and oral cavity and a few others [1, 2].

Most of the PS that have been used for cancer treatment have a macrocyclic framework based on the tetrapyrrole backbone typical of porphyrins, chlorins, bacteriochlorins and phthalocyanines. This contribution to Macrocycle Fest will review the different molecular features of the PS and their effect in PDT, aiming to better understand how to optimize their design.

## 2. Photosensitizer excitation mechanisms “unmasked”

The ground state PS has two electrons with opposite spins (singlet state) in the lowest energy molecular orbital. Following the absorption of light (photons), one of these electrons is boosted into a higher-energy orbital but retains its spin (first excited singlet state). This is a short-lived (nanoseconds) species and can lose its energy by emitting light (fluorescence) or by internal conversion into heat. The fact that most PS are fluorescent has led to the development of sensitive assays to quantify the amount of PS in cells or tissues, and allows in vivo fluorescence imaging in living animals or patients to measure the pharmacokinetics and distribution of the PS. The excited singlet state PS may also undergo the process known as intersystem crossing whereby the spin of the excited electron inverts to form the relatively long-lived (microseconds to milliseconds) excited triplet-state that has both electron spins parallel. The long life of the triplet state is attributed to the relative rarity of other triplet molecules with which it can interact.

The PS excited triplet can undergo three broad kinds of reactions that are usually known as type I, type II and type III (see Jablonski diagram in figure 1). Firstly, in a type I reaction, the triplet PS can gain an electron from a neighboring reducing agent. In cells these reducing agents are commonly either nicotinamide adenine dinucleotide (NADH) or NAD-phosphate, reduced form (NADPH). The PS is now a radical anion bearing an additional unpaired electron ( $PS^{\bullet-}$ ). Alternatively two triplet PS molecules can react together involving intermolecular electron transfer to produce a pair consisting of a radical cation and a radical anion. The PS radical anions may further react with oxygen to carry out an electron transfer to produce reactive oxygen species, in particular superoxide anion. The damaging effects of superoxide are relatively mild, however it can cause much more oxidative damage when it reacts with itself to produce hydrogen peroxide and oxygen, in the process called "dismutation". Hydrogen peroxide, can add to an organic (carbon-containing) substrate and result in an oxidizing "chain reaction". This is common in the oxidative damage of fatty acids and other lipids. Hydrogen peroxide is important in the production of the highly reactive hydroxyl radical ( $HO^{\bullet}$ ), by a second one-electron reduction mediated by  $PS^{\bullet-}$ . Superoxide will additionally react with nitric oxide ( $NO^{\bullet}$ ) (also a radical) to produce peroxynitrite ( $OONO^-$ ), another highly reactive molecule that can oxidize many functional groups and can also nitrate proteins on tyrosine residues.

In a type II reaction, the triplet PS can transfer its energy directly to molecular oxygen (itself a triplet in the ground state), to form excited-state singlet oxygen. Type II processes are thought to best preserve the PS molecular structure in a repeatedly photoactivatable state, and in some circumstances a single PS molecule can generate 10,000 molecules of singlet oxygen. The PS can in some circumstances also react with the singlet oxygen it produces in a process known as oxygen-dependent photobleaching.

Singlet oxygen generated during type II photochemical reactions, is believed to be the most important molecule responsible for PDT-induced cellular damage [7, 8]. However, because of the high reactivity and short half-life of singlet oxygen only molecules and structures that are proximal to the area of its production (areas of PS localization) are directly affected by

PDT. The half-life of singlet oxygen in biological systems is <40 ns, and, therefore, the radius of the action of singlet oxygen is of the order of 20 nm [9].

A less common pathway is known as type III and here the triplet state PS reacts directly with a biomolecule thus destroying the PS and damaging the biomolecules. This pathway can occur in the absence of oxygen.

Type I and type II reactions can occur simultaneously, and the ratio between these processes depends on the type of PS used, the concentrations of substrate and oxygen and both singlet oxygen as well as other radicals and ROS, including  $O_2^{\bullet-}$ ,  $H_2O_2$ ,  $^{\bullet}OH$  and  $NO$  have been detected in cells and tissues exposed to PDT treatment [10] supporting the evidence for their active role in PDT induced cytotoxic effects [8, 11].

The aforementioned ROS, together with singlet oxygen are oxidizing agents that can directly react with many biological molecules. Amino acid residues in proteins are important targets that include cysteine, methionine, tyrosine, histidine, and tryptophan [12, 13].

DNA can be oxidatively damaged at both the nucleic bases and at the sugars that link the DNA strands by oxidation of the sugar linkages, or cross-linking of DNA to protein (a form of damage particularly difficult for the cell to repair).

### 3. A photosensitizer checklist

The characteristics of the ideal PS have been discussed in recent reviews [14, 15]. PS should have low levels of dark toxicity to both humans and experimental animals and a low likelihood of adverse pharmacological effects upon administration such as hypotension (decreased blood pressure) or allergic reactions. PS should absorb light in the red or far-red wavelength regions in order for the tissue damaging effect to reach as deep as possible. It is known that both absorbance and scattering of light are minimized at longer which penetrate tissue deeper. Absorption bands at shorter wavelengths have less tissue penetration and are more likely to lead to skin photosensitivity (the power in sunlight drops off at  $\lambda > 600\text{-nm}$ ). Absorption bands at high wavelengths ( $> 800\text{-nm}$ ) mean that the photons will not have sufficient energy for the PS triplet state to transfer energy to the ground state oxygen molecule to excite it to the singlet state. They should have relatively high absorption bands ( $> 20,000\text{ M}^{-1}\text{cm}^{-1}$ ) to minimize the dose of PS needed to achieve the desired effect. Synthesis of the PS should be relatively easy and the starting materials readily available to make large-scale production feasible. The PS should be a pure compound with a constant composition and a stable shelf life, and be ideally water soluble or soluble in a biocompatible drug-delivery vehicle. It should not aggregate unduly in biological environments as this reduces its photochemical efficiency. The pharmacokinetic elimination from the patient should be rapid i.e. less than one day to avoid the necessity for post-treatment protection from light exposure and prolonged skin photosensitivity. A short interval between injection and illumination is desirable to facilitate outpatient treatment that is both patient-friendly and cost-effective. Pain on treatment is undesirable, as PDT does not usually require anaesthesia or heavy sedation. Although high PDT activity is generally thought to be a good thing, it is possible to have excessively powerful PS that are considered

to be “unforgiving”. With limitations in the effectiveness of both PS and light dosimetry, highly active PS may easily permit treatment overdosage when surrounding normal tissue is damaged as well as the target tumor. It is at present uncertain whether it is better to have a PS “tailored” to a specific indication and to have families or portfolios of PS for various specific diseases or patient types, or alternatively to seek one PS that works against most diseases. For cancer treatment it has been thought that an ideal PS should selectively accumulate in tumors after intravenous injection. Although the exact mechanisms for this “tumor-localizing effect” are not completely understood, some PS can achieve a 5:1 or higher accumulation in tumors compared to surrounding normal tissue. Lastly a desirable feature might be to have an in-built method of monitoring PS dosimetry localization and following response to treatment by measuring in vivo fluorescence and its loss by photobleaching

#### 4. Tetrapyrrole macrocycles as PS

Out of the plethora of chemical compounds that have been described as effective PDT mediators the tetrapyrrole derivatives are the group that has been most extensively studied. Their structural characteristic is based on four pyrrole rings connected by methine bridges in a cyclic configuration, sometimes associated with a centrally coordinated atom that is usually metallic (see Figure 2). Tetrapyrroles usually have a relatively large absorption band in the region of 400-nm known as the Soret band, and a set of progressively smaller absorption bands as the spectrum moves into the red wavelengths known as the Q-bands (Figure 1). Naturally occurring porphyrins are fully conjugated (non-reduced) tetrapyrroles and vary in the number and type of side groups particularly carboxylic acid groups (uroporphyrin has eight, coproporphyrin has four and protoporphyrin has two). Porphyrins have the longest wavelength absorption band in the region of 630 nm and this band tends to be small. Chlorins are tetrapyrroles with the double bond in one pyrrole ring reduced. This means that the longest wavelength absorption band shifts to the region of 650–690 nm and increases several-fold in height; both these factors are highly desirable for PDT. Bacteriochlorins have two pyrrole rings with reduced double bonds, and this leads to the absorption band shifting even further into the red, and increasing further in magnitude. Bacteriochlorins may turn out to be even more effective PS than chlorins, but with relatively few candidate molecules and some questions about the stability of these molecules upon storage and a tendency to rapid photobleaching this remains to be seen. There are a set of classical chemical derivatives generally obtained from naturally occurring porphyrins and chlorins that include such structures as purpurins, pheophorbides, pyropheophorbides, pheophytins and phorbins some of which have been studied (a few extensively) as PS for PDT.

The tetrapyrrole nucleus frequently holds a co-coordinated metal atom, but it has been found that only diamagnetic metals, that do not contain unpaired electrons, such as (Zn, Pd, In, Sn, Lu) allow the tetrapyrrole to retain its photosensitizing ability, while paramagnetic metals such as (Fe, Cu, Gd) do not [16]. Many of these compounds are lipophilic and some are even insoluble in water. These compounds must either be delivered in an emulsion or else incorporated in liposomes.

Hematoporphyrin derivative or Photofrin **1** was the first PS to be studied in detail [17–21] Its chemical structure showed a significant variation between batches and attempts to fractionate it into its individual component molecules frequently yielded mixtures as complicated as the starting material [22, 23]. Other significant deficiencies include: i) long lasting skin photosensitivity for up to eight weeks after administration, ii) the lack of a reasonably-sized absorption band > 650 nm, and iii) the fact that its tumor-localizing properties are not as consistent as it is desired. Despite these shortcomings Photofrin continues to be the most widely used PS in both experimental and clinical settings even today.

## 5. Structure-function relationship: lipophilicity, solubility, aggregation, delivery vehicles

Huang et al. [24] tested twelve new, stable synthetic bacteriochlorins bearing a range of peripheral substituents, for PDT activity and their ability to kill HeLa human cervical cancer cells as to create a quantitative relationship between the structure and function of these photosensitizers. The twelve bacteriochlorins all varied in their polarity values. From these values three compounds were shown to be lipophilic, four compounds could be grouped together as amphipathic and the remaining five compounds were more polar [24]. Molecules in each of these three groups contain specific structural motifs unique to each polarity value set. For example (structures shown in scheme 1), one bacteriochlorin in the lipophilic group includes four hydroxyl groups and two tertiary nitrogen atoms, thus giving it an electron-rich and basic character **2**, while a bacteriochlorin in the amphipathic group had a symmetrical structure with two phenyl rings substituted with hydroxyl groups **3**. Some of these bacteriochlorins can also differ via their overall charge such as the bacteriochlorin containing four quaternized nitrogen atoms will be highly cationic **4**, while the bacteriochlorin with two carboxyl groups will be negatively charged **5**.

The measured partition coefficient (mLogP) values reflected the hydrophobicity and hydrophilicity of the compounds. Like any other PS, there are several confounding factors that are to be expected to influence the effectiveness of the bacteriochlorins in PDT. In order to isolate the relationship between structure and function in these bacteriochlorins, the contribution of cellular uptake to PDT efficacy was accounted for through a parameter named 'survival fraction/unit uptake'. A quantitative structure-activity relationship (QSAR) was determined for several different parameters, all of which affected PDT effectiveness (cellular uptake, cell killing/unit uptake and LD50,). This was plotted against parameters of lipophilicity, namely mLogP and cLogP. There was a strong correlation between 'cell killing/unit uptake and mLogP ( $R^2 = 0.94$ ). For instance the relative effectiveness of the four compounds shown in scheme 1 was **1** > **2** > **3** > **4** spanning over three orders of magnitude in relative activity.

Besides cellular uptake, the bacteriochlorins varied between one another based on two main factors. The first was attributed to the differences in the subcellular localization in the organelles (lysosomes, endoplasmic reticulum, mitochondria, etc.). The second variation was caused by the type of photochemical mechanism (either Type I or Type II). Changes in

hydrophobicity of the bacteriochlorins could affect the photochemical mechanism and could affect subcellular localization. It was found that the more hydrophobic a PS is, will encourage it to localize more in the mitochondria and endoplasmic reticulum due to the large proportion of lipid bilayers found in these respective organelles. Damage to these cellular organelles via PDT-induced ROS toxicity is much more likely to cause apoptosis when compared to other organelle damage, such as lysosomes, where hydrophilic PS are located. Hydrophobic PS tend to more utilize Type I photochemistry and create hydroxyl radicals when surrounded by an aqueous environment. However, the hydrophilic PS undergo Type II photochemistry and create more singlet oxygen, and in turn localize in less critical organelles which were once thought to be lysosomes, until Oleinick's group showed that some phthalocyanine-based PS are highly active when localized in lysosomes [25]. These relationships help explain the strong correlation between phototoxicity/unit uptake and mLogP. The most active of these photosensitizers have both low dark toxicity and high phototoxicity [24].

In order to penetrate better through cell membranes by diffusion, many PS are not water soluble, but rather very hydrophobic. To overcome aggregation in aqueous or polar environments, delivery vehicles such as liposomes, lipoproteins or micelles are often necessary for delivery of these hydrophobic PS [26]. Commonly used as a delivery vehicle for many water insoluble drugs, Cremophor EL (CrEL) is a nonionic detergent in which a portion of the delivered drug is aggregated and then disaggregates rapidly *in vivo* [27]. Although CrEL is widely considered to be of low toxicity, adverse side-effects have occurred such as allergic reactions and peripheral neuropathy [28, 29]. CrEL micelles were used as a nano-delivery vehicle to transport the hydrophobic bacteriochlorins **6** and **7** (scheme 1) by increasing the solubility while minimizing aggregation of the compound until it was taken up into the cells where the compound can then localize into the hydrophobic compartments [30]. The enhanced PDT activity and bacteriochlorin solubility through the use of CrEL micelles was measured by LD50 values for killing HeLa cancer cells. Since the LD50 values significantly improved when using CrEL versus base bacteriochlorin, we can conclude that the use of CrEL as a delivery vehicle for transportation of bacteriochlorins to cells leads to a stronger PDT effect [31]

## 6. Charge (cationic, anionic, neutral)

Nitzan et al. [32] looked at the structure-activity relationship (specifically at charge) of porphyrins as PS for PDT in various bacteria. Effects of uncharged (o-tetrahydroxyphenyl porphyrin, THPP, m-THPP and p-THPP **8**), cationic (5,10,15,20-tetra [4-N-methylpyridyl] porphyrin, TMPyP) **9**, and anionic (5,10,15,20-tetra [4-sulfonatophenyl porphyrin], TPPS4) **10** (Scheme 2) on *Staphylococcus aureus* and *Escherichia coli* bacteria inactivation were examined. Nitzan showed that uncharged porphyrins induced antibacterial activity in *S. aureus* when used alone, and in *E. coli* while in the presence of the membrane disorganizing peptide polymyxin B nonapeptide (PMNP). The cationic compound **9** showed a great amount of photoactivity toward Gram-positive bacteria and was also effective on Gram-negative cells. The anionic compound **10** showed no activity at all on either the Gram-positive cells or the Gram-negative cells. For the cationic compound **9**, the high photoactivity was caused by the electrostatic attraction between the positively charged PS

molecule and the negative charge along the membrane of the Gram-positive bacterial cells to which they were targeted. Conversely, the lack of photoactivity in the anionic compound **10** and neutral compound **8** was due to electrostatic repulsion caused by the charged PS and that of the target cell membrane (both negatively charged). For the Gram-negative cells, the inactivity here was caused by the electrostatic binding to the positively charged peptide PMNP, which facilitated membrane disorganization, yet has no effect on cell viability.

The effects of varying the molecular charge are less clear-cut when it comes to cancer cells. Certainly cationic compounds are much more likely to be effective than anionic compounds. Anionic compounds such as tetrasulfonates, tetracarboxylic acids (and octacarboxylic acids such as uroporphyrin) have a very poor uptake into cells. This is probably due to these highly anionic compounds fail to bind to anything on the cell surface. Consequently their only way of being taken up is by fluid phase endocytosis, a fairly inefficient process compared to transmembrane diffusion or adsorptive endocytosis. Moreover if these compounds are taken up by fluid phase endocytosis they will be localized in the aqueous interior of the lysosomes, rather than the lipid membranes comprising the walls of the lysosomes. When ROS are photogenerated in the aqueous core of the lysosomes, the likelihood of them breaking the lysosomes open to release damaging enzymes like cathepsins, is much lower than when the PS are actually located within the lysosomal membranes. On the other hand cationic PS tend to bind to the negatively charged residues on the cell surface and trigger adsorptive endocytosis. Cationic PS are also localized in lysosomes, but this time the PS are still attached to the lysosomal membranes and when they are photoactivated, the likelihood of the lysosomal membranes being ruptured is much higher. Moreover it has been shown that lipophilic cationic compounds can selectively localize in mitochondria [33]. When these compounds are photoactivated the mitochondria are damaged releasing cytochrome c and triggering mitochondrial apoptosis (see figure 3) [34].

## 7. Molecular asymmetry

It has been observed by studying many series of compounds, that for two isomeric structures the one that has a higher degree of molecular asymmetry will be more effective than the more symmetric one. This was illustrated by the grouping of aluminum sulfonated phthalocyanines. It has previously been established that the mono- and di-sulfonated compounds were more effective than the tri- and tetra-sulfonated compounds in vitro, but that the mono-sulfonated compound lost its activity in vivo [35]. The di-sulfonated compound exists as a pair of isomers, the symmetrical (opposite) AlPCS<sub>2</sub>-o **11**, and the asymmetrical (adjacent) AlPCS<sub>2</sub>-a **12** (scheme 2). It was shown by Paquette et al [36, 37] that the asymmetrical isomer AlPCS<sub>2</sub>-a was more powerful. The explanation for this observation was that the compound could penetrate into lipid bilayer membranes due to its hydrophobic non-sulfonated side, but could not entirely diffuse through the membranes due to its polar sulfonated side anchoring it in the aqueous environment. This principle of being anchored in lipid membranes was put to use by Berg's group in a large body of work dedicated to photochemical internalization (PCI) [38]. PCI is a drug-delivery technology in which a PS such as **12** is administered in combination with a macromolecule (e.g. a ribosome inactivating protein, RIP) that would be expected to be localized in endosomes/lysosomes.



Since the AIPCS<sub>2</sub>-a is localized in lysosomal membranes a small amount of light can break open the lysosomes releasing the RIP to damage the ribosomes and kill the cell [39].

Another example of the influence of molecular asymmetry was obtained with bacteriochlorins [40] (Scheme 3). We were able to compare a monosubstituted cationic compound **13** [41] with a disubstituted cationic BC **14** that had been prepared and studied for antimicrobial photodynamic inactivation in another study [42]. The results of PDT of HeLa cancer cells showed that the monosubstituted cationic **13** was three orders of magnitude (1000 times) more powerful than the corresponding di-substituted cationic **14**. The explanation of this remarkable finding undoubtedly resides in the amphiphilic character of the mono-substituted bacteriochlorins. Insertion of tetrapyrrole photosensitizers into cell membranes may be critically involved in the sub-cellular mechanism [43] and it is expected that amphiphilic, mono-substituted bacteriochlorins would do so much more easily than the symmetrical disubstituted bacteriochlorins

## 8. Pharmacokinetics and biodistribution

Water solubility of PS is a key determinant in their mechanism of administration, affecting the pharmacokinetics and biodistribution. The anticancer action of PDT is a consequence of a low-to-moderate selective degree of PS uptake by proliferative malignant cells and direct cytotoxicity and antivascular action that impairs the blood supply to the area of light exposure. [44]. Accordingly, a major aim is to select an appropriate drug-light interval where the PS uptake in tumor mass is maximized, while minimizing the presence of PS in surrounding healthy tissues. Although much research has been undertaken in this area, the structural features of the molecule necessary to make the ideal PS are still unknown. Tumor uptake relies on the hydrophilicity/hydrophobicity of these molecules. It is likely that due to the higher expression of low density lipoprotein (LDL) receptors in tumors in comparison to other cell types, LDL-bound lipophilic PS will be more prone to be internalized by LDL-receptor mediated endocytosis, than hydrophilic PS, which mainly bind to serum proteins such as albumin and tend to localize in the vascular stroma. Many second generation PS have been designed to have rather low water-solubility based on the higher uptake in tumors and thus a better PDT outcome. Table 1 lists a representative sample of tetrapyrrole-based PS that have been used in animal experiments *in vivo*, and some of which have been used clinically. It should be noted that the doses given are those that have been used in animal studies, and are not necessarily the same as the doses used clinically.

One clinically approved PS is Foscan®, whose active compound is meta-(tetra-hydroxyphenyl)chlorin (mTHPC) **20**. I.V. injection showed the initial presence of mTHPC in plasma 10–20 min after administration, followed by a steady increase to a maximal value at 4–6 hr after injection and being finally cleared over the following 24–70 hr [45, 46]. Meso-tetra[3-(N,N-diethyl)aminomethyl-4-methoxy]phenyl-chlorin (TMPC) **34** showed a reduced initial accumulation in tumor 1hr post administration compared to liver, skin and serum, which then increased at 3hr; yet, it was still higher in liver and serum [47]. Overall clearance was rapid, nearly eliminated by 12hr and negligible after 24hr; removal from tumor tissue was slower, possibly due to drug protonation in the acidic environment of tumors which then becomes more lipophilic, engulfment by macrophages or poor lymphatic drainage [47].

Another widely used hydrophobic chlorin-based photosensitizer is SnET2 (tin etiopurpurin) **19**. It displayed intravascular localization 1 hr after I.V. injection in rabbits showing selectivity for the non-pigmented ciliary body epithelium by 24 hr [48]. Maximal PS uptake was found in mice liver ( $4.97 \pm 0.73 \mu\text{g/g}$ ) 24hr after I.V. injection, and present in minor levels ( $0.41 \pm 0.18 \mu\text{g/g}$ ) compared to other organs observed in the study [49]. This was consistent with distribution found in the study carried out by Kessel et al. in 1992, liver > skin > tumor [50]. Despite previous hypothesis explaining biodistribution of SnET2 founded on its affinity for LDL and the amount of LDL receptor in the different organs, the authors could not reach an ultimate conclusion regarding the role of LDL in PS biodistribution [50]. Silicon phthalocyanine (Pc4) **28** is a relatively hydrophobic PS whose distribution has been compared administered I.V. either diluted in NaCl or else using vehicle consisting of PEG:Tween [51]. 40mg/kg injection of PS resulted in peak plasma concentrations 5 minutes after injection and it was still present at least up to 168 hr. If doses were reduced to 10 and 2 mg/kg a 5 minute peak was also found, but PS presence only remained up to 120hr (both delivery vehicles for 10mg/kg and only PEG:Tween for the lowest dose). Pc4 was detected in all tissues studied (including brain, lung, liver, kidney, skeletal muscle, skin, heart, spleen, and abdominal fat) and had long persistence. The use of PEG:Tween also reduced PS levels in the brain. In addition, clearance of Pc4 was not likely to happen through renal pathways based on the low levels of PS found in urine samples.

Among hematoporphyrin derivatives, commercially available Photogem® **15** resulted in a fast accumulation in liver (9 min post injection), followed by skin (400 min) and being slowest in kidney tissue (600 min). The same clearance pattern was followed [52]. Biodistribution of the benzoporphyrin derivative, verteporfin, was compared in 5 studies involving human subjects administered I.V. [53]. Initial rapid distribution throughout the body 1–3 hr after injection was followed by an elimination of up to 6 hours. 91% of the PS injected appeared to be bound to different lipoproteins, correlating with the highest clearance by the liver (99.5%), the major reticuloendothelial system (RES) organ with an elevated number of LDL-receptors [53]. This confirms previous reports, which correlated the amount of LDL receptors in the different organs with the porphyrin biodistribution. Talaporfin **18**, (N-aspartylchlorin(e6), NPe6, mono-L-aspartyl-chlorin e6 –MACE–, LS11 or Laserphyrin) was studied for choroidal neovascularization [54]. Presence of the PS in the experimental animal bloodstream was seen as early as 1 minute after injection, finding a peak between 20 and 60 minutes and then being rapidly cleared [54]. Previous studies had shown the highest tissue distribution in liver followed by spleen and kidney before observing the tumor peak [55]. Plasma fractions showed similar presence of the PS 30 minutes after administration up to 24 hr and indicated the highest affinity for HDL and lowest for LDL [55]. Expansion of the porphyrin rings in a tetrapyrrole resulted in Lutex **23**, “a texaphyrin macrocycle” comprising a penta-aza core, which shifts absorption to longer wavelength light being able to reach deeper tissues. Accumulation of lutetium(III) texaphyrin complex in normal tissues was very low, only detectable in tumor, liver, spleen, muscle and kidney. It was prevalent in tumor exhibiting an accumulation peak at 3 days (233.1 lg/g wet tissue); despite also finding maximal uptake in liver at this point, the tumor to liver ratio was low (0.102) [56]. During a comparison between Photofrin and aluminum phthalocyanine tetrasulfonate (AlPcS<sub>4</sub>) **17** an increased accumulation in plasma was seen 30 minutes after

administration, which was then more rapidly cleared with the latter compound [57]. The authors explained the differences in pharmacokinetics by the greater lipophilicity of Photofrin components. Tumor concentration peaked significantly earlier in the case of ALPcS<sub>4</sub>, at 30 minutes as opposed to 12–72 hr which was the case for Photofrin, which also exhibited a nearly 11-fold longer half life (8). PS levels in RES organs were also significantly higher for Photofrin, these were high even 90 hr after injection [57].

Metalation of the PS core has previously demonstrated to have a great influence on its photophysical properties. A palladium-metallated bacteriopheophorbide molecule, TOOKAD (WST09, micelle-based) **25**, is undergoing clinical trials for prostate cancer treatment where external beam radiation therapy has failed [58]. More recently a water-soluble derivative was obtained (WST11) **26**, which forms a non-covalent complex of the compound with human serum albumin after injection; until these are cleared, they will both remain in circulation, thus limiting the photosensitizing effect to the vasculature. As a matter of fact, clearance is fast, first from circulation followed by the liver [58, 59]. I.V. injection of the polar WST11 derivative showed the highest levels found in blood immediately post-injection, then peaks were found in liver lung, kidney and spleen and as soon as 60 minutes after injection it was completely cleared from all tissues except for the lungs, where traces were found 24 hr post I.V. [59]. This results in a very short therapeutic window of the compounds. Structural differences between TOOKAD and TOOKAD soluble have been proposed to be the cause of differences in distribution and pharmacokinetics between them. Similarly, WST09 was only seen in vasculature, showing a peak in plasma as soon as 5 minutes post administration and being completely cleared after 3hr [60]. However, WST09 levels in liver and kidneys were initially high and gradually decreased up to 24hr and 9hr respectively. This indicates binding to RES organs, a feature of hydrophobic compounds. No localization in tumor, skin or muscle has been reported with either compound; suggesting a higher PDT effect is likely to be found in highly vascularized tumors [60]. In 2015, benzyloxy-substituted zinc(II) pheophorbide-a (Zn-PH-A) showed a slow distribution and followed renal and hepatobiliary elimination [61]. The same group also tested a Cu-chlorophyll derivative, copper(II) benzyloxypheophorbide-a (Cu-PH-a) confirming a renal and hepatobiliary clearance, based on the increase of levels found in the intestines upon reduction of levels in the liver 2 hr after administration [62]. Again, high liver uptake was related to lipophilicity of the PS [62]. The modified porphyrin IY69 [(5-phenyl-10,15-bis(4-carboxylatometoxyphenyl)-20-(2-thienyl)-21,23-dithiaporphyrin)] **32** showed high uptake by liver and kidney, reaching a peak at 24hr in the former. Tumor tissue exhibited higher accumulation than other tissues and maximal uptake was seen at 72hr [63].

Imaging of Photochlor®, 2-1-hexyloxyethyl-2-devinyl pyropheophorbide-a (HPPH) **24** in mice bearing a tumor in the ear showed a 2 to 3 fold tumor to skin ratio [64]. In a different study, maximal uptake of this PS was found in liver followed by the other organs measured, at similar levels to tumor, significant retention even at 48 hr [65].

Hydrophilic photosensitizers are easier to prepare for *in vivo* administration. These compounds will be less prone to opsonization and uptake by RES organs and will show more rapid distribution and faster clearance. Sinoporphyrin sodium (DVDMS) **16** is a highly water-soluble novel PS studied for PDT-treatment of different cancers. A rapid reduction in

levels of this PS in the circulation was observed during the first 6 hr [66], which was then stabilized at low levels by 72 hr. Maximal accumulation was found in most organs within the first 2hr, including spleen, liver and kidney, then reduced by 24 hr [66]. As for tumors, accumulation increased 6–12hr, reaching a peak at this point, detecting selectivity compared to muscle and skin. Very low amounts were seen at 48–72hr [66]. Cationic salts of bacteriochlorin such as meso-tetrakis (N-alkyl-3-pyridyl)bacteriochlorin **31** showed accumulation peaks in tumors as early as after 15–30 min after administration, followed by progressive clearance, with only 7.3%–26.3% remaining 96 hr after injection [67]. Tumor-specificity was confirmed by the tumor/skin and tumor/muscle ratios [67]. Studies with radachlorin (Chlorin e6 derivative) **27** in 2014 [68] showed gradual accumulation in tissues (tumor sites among these) 3–6 hr post administration. At 12 hr it was still visible in tumors, while decay in other organs had already started at 6 hr. Elimination from malignant sites was observed 24 hr post administration and levels were insignificant 24 hours after that [68].

Liposomes increase the interaction between their drug load and tumor cells through LDL receptors and the EPR effect. Nonetheless, liposomes can suffer some recognition by the RES and be rapidly removed from circulation; therefore, coating strategies are sometimes followed, resulting in so-called “stealth” liposomes. Delivery of ZnPc(OCH<sub>3</sub>)<sub>4</sub> **29** was enhanced using liposomes as indicated by the earlier presence in tumor and selectivity, 24–72 hr after administration [69]. I.P. and I.V. injections were compared, finding a higher uptake after the former, suggesting rapid RES activity. The highest fluorescence levels were still recorded in RES organs spleen, kidney and liver; peaks in different tissues were observed 72 hr after administration [69]. A comparison between free indocyanine green and liposomal formulation of the same photosensitizer [70] **33**, concluded a faster elimination of the former from circulation, as early as 4hr after injection; while a higher presence of the liposomal formulation was found in the tumor mass up to 48 hr. Both were present in tumor, heart, liver, spleen and kidneys and in the lungs, the liposomal indocyanine green was significantly higher [70].

Studies with Foslip, a liposomal formulation of mTHPC [unilamellar dipalmitoylphosphatidylcholine / dipalmitoylphosphatidylglycerol (DPPC/DPPG)] **21** displayed a rapid clearance in plasma, while its accumulation increased progressively in tumors, reaching a plateau 6–15 hr after injection followed by a peak uptake at 72hr which was not significantly different to 6hr [71]. Previous studies using non-liposomal mTHPC, resulted in maximal tumor uptake 24–48hr after injection [72]. Overall uptake, biodistribution and final elimination of Foslip (0.13hr, 4.31 hr and 35.7 hr half lives) was faster than that exhibited by Foscan® [72, 73]. Foscan® current 96hr drug light interval (DLI) could be shortened via the use of liposomally-encapsulated mTHPC. A similar study was performed using mTHPC encapsulated in liposomes with different degrees of PEGylation (either 2% or 8%) [73] to make a formulation called Fospeg **22**. PEG (polyethylene glycol) can sterically stabilize and increase the hydrophilicity of liposomes, reducing the likelihood of opsonization and clearance. A reduced accumulation and rapid clearance of mTHPC in 2% PEG-liposomes in the liver was observed; this could be due to an increase in hydrophilicity of the system [73]. 8% PEGylated liposomes were not significantly different to Foscan®. There was greater presence in vasculature of both 2% and

8% PEG-liposomes than Foslip or Foscan® as concluded by  $V_D$  values [73]. PEGylation significantly reduced uptake by RES, in an inversely proportional to the degree of PEGylation of liposomes (34.6 and 14.7 ml/kg for 2% and 8% respectively) [73]. PEGylation significantly affected methoxypolyethylene glycol pheophorbide a (mPEG-Pba) 30 distribution in tissues, increasing accumulation 8–13 times compared to free PS. Body distribution of mPEG-Pba was rapid and it was found throughout the different tissues only 1hr after injection, showing maximal dissemination 3–5 hr and persisting in lower amounts 24–48 hr; while free Pba remained closely located to the injection site. Besides, uptake of mPEG-Pba by tumors was approximately 3 times that of free Pba [74, 75].

## Conclusion

Traditional drug design methodologies have not been extensively employed in design of PS for PDT. Lipinski's rule of five is never mentioned in this regard. Perhaps that is not too surprising, because Lipinski's rule was mainly designed to screen whether compounds could function as orally administered drugs that could be absorbed in the small intestine, rather than intravenous injection which is the common mode of administration in PDT, especially when the PS are used for treating cancer. Moreover a molecular weight < 500 is an unattainable criterion is most of the tetrapyrrole macrocyclic structures used in PDT, where molecular weights tend to start at 600 and go up from there. The other important traditional design requirement is likewise not particularly relevant in PDT. Since there are no easily-defined target molecules (such as receptors and enzymes) for the drug to bind to, computer-aided molecular modeling is not often used. Instead the requirements for highly active PS lie in completely different areas as discussed in section 3, with much more emphasis on optical properties (wavelength, extinction co-efficient and triplet yield).

The present review has shown that in general non-water soluble PS that require a drug-delivery formulation to be administered to cells or animals do perform better than water soluble compounds. More in vivo studies are necessary to clarify the relationship between chemical structures and tumor-selective accumulation mechanisms in order to develop a better PS. This will have a major impact in the selection of therapeutic windows, drug-light intervals for each specific sensitizer. Shorter DLIs would allow drug doses to be reduced, decreasing the possibility of skin sensitivity and shortening the period of light avoidance to limit the main side-effect of phototoxicity.

## Acknowledgments

Michael R Hamblin was supported by US NIH grant R01AI050875. Alejandra Martinez De Pinillos Bayona was supported by the Bogue Research Fellowship, from UCL

## References

1. Henderson BW, Dougherty TJ. How does photodynamic therapy work? *Photochem Photobiol.* 1992; 55(1):145–157. [PubMed: 1603846]
2. Agostinis P, et al. Photodynamic therapy of cancer: an update. *CA Cancer J Clin.* 2011; 61(4):250–281. [PubMed: 21617154]
3. Levy JG. Photodynamic therapy. *Trends Biotechnol.* 1995; 13(1):14–18. [PubMed: 7765800]

4. Vrouenraets MB, et al. Basic principles, applications in oncology and improved selectivity of photodynamic therapy. *Anticancer res.* 2002; 23(1B):505–522.
5. Dougherty TJ. An update on photodynamic therapy applications. *J Clin Laser Med Surg.* 2002; 20(1):3–7. [PubMed: 11902352]
6. Oleinick NL, Evans HH. The photobiology of photodynamic therapy: cellular targets and mechanisms. *Radiat Res.* 1998; 150(5 Suppl):S146–S156. [PubMed: 9806617]
7. Weishaupt KR, Gomer CJ, Dougherty TJ. Identification of singlet oxygen as the cytotoxic agent in photoinactivation of a murine tumor. *Cancer Res.* 1976; 36(7 PT 1):2326–2329. [PubMed: 1277137]
8. Henderson BW, Miller AC. Effects of scavengers of reactive oxygen and radical species on cell survival following photodynamic treatment in vitro: comparison to ionizing radiation. *Radiat Res.* 1986; 108(2):196–205. [PubMed: 3097749]
9. Moan J, Berg K. The photodegradation of porphyrins in cells can be used to estimate the lifetime of singlet oxygen. *Photochem. Photobiol.* 1991; 53(4):549–553. [PubMed: 1830395]
10. Hariharan PV, Courtney J, Eleczko S. Production of hydroxyl radicals in cell systems exposed to haematoporphyrin and red light. *Int J Radiat Biol Relat Stud Phys Chem Med.* 1980; 37(6):691–694. [PubMed: 6968301]
11. Chekulayeva LV, et al. Hydrogen peroxide, superoxide, and hydroxyl radicals are involved in the phototoxic action of hematoporphyrin derivative against tumor cells. *J Environ Pathol Toxicol Oncol.* 2006; 25(1–2):51–77. [PubMed: 16566710]
12. Grune T, et al. Protein oxidation and proteolysis by the nonradical oxidants singlet oxygen or peroxyxynitrite. *Free Radic. Biol. Med.* 2001; 30(11):1243–1253. [PubMed: 11368922]
13. Midden WR, Dahl TA. Biological inactivation by singlet oxygen: distinguishing O<sub>2</sub>(<sup>1</sup>Δ<sub>g</sub>) and O<sub>2</sub>(<sup>1</sup>Σ<sub>g</sub><sup>+</sup>). *Biochim. Biophys. Acta.* 1992; 1117(2):216–222. [PubMed: 1525183]
14. Detty MR, Gibson SL, Wagner SJ. Current clinical and preclinical photosensitizers for use in photodynamic therapy. *J. Med. Chem.* 2004; 47(16):3897–3915. [PubMed: 15267226]
15. Allison RR, et al. Photosensitizers in clinical PDT. *Photodiag Photodynam Ther.* 2004; 1:27–42.
16. Rosenthal I, et al. The role of molecular oxygen in the photodynamic effect of phthalocyanines. *Radiat Res.* 1986; 107(1):136–142. [PubMed: 3737875]
17. Kessel D. Probing the structure of HPD by fluorescence spectroscopy. *Photochem Photobiol.* 1989; 50(3):345–350. [PubMed: 2780824]
18. Kessel D, et al. Probing the structure and stability of the tumor-localizing derivative of hematoporphyrin by reductive cleavage with LiAlH<sub>4</sub>. *Cancer Res.* 1987; 47(17):4642–4645. [PubMed: 3621158]
19. Kessel D, Thompson P. Purification and analysis of hematoporphyrin and hematoporphyrin derivative by gel exclusion and reverse-phase chromatography. *Photochem Photobiol.* 1987; 46(6):1023–1025. [PubMed: 2964039]
20. Kessel D, et al. Chemistry of hematoporphyrin-derived photosensitizers. *Photochem Photobiol.* 1987; 46(5):563–568. [PubMed: 2964649]
21. Kessel D. Photosensitization with derivatives of haematoporphyrin. [Review]. *Int J Radiat Biol Relat Stud Phys Chem Med.* 1986; 49(6):901–907. [PubMed: 2940198]
22. Kessel D. On the purity and definition of oligomeric HPD formulations. *J Photochem Photobiol B.* 1989; 3(4):637–638. [PubMed: 2507762]
23. Kessel D. Components of hematoporphyrin derivatives and their tumor-localizing capacity. *Cancer Res.* 1982; 42(5):1703–1706. [PubMed: 7066890]
24. Huang YY, et al. In vitro photodynamic therapy and quantitative structure-activity relationship studies with stable synthetic near-infrared-absorbing bacteriochlorin photosensitizers. *J Med Chem.* 2010; 53(10):4018–4027. [PubMed: 20441223]
25. Rodriguez ME, et al. Structural factors and mechanisms underlying the improved photodynamic cell killing with silicon phthalocyanine photosensitizers directed to lysosomes versus mitochondria. *Photochem Photobiol.* 2009; 85(5):1189–1200. [PubMed: 19508642]
26. Konan YN, Gurny R, Allemann E. State of the art in the delivery of photosensitizers for photodynamic therapy. *J Photochem Photobiol B.* 2002; 66(2):89–106. [PubMed: 11897509]

27. Sparreboom A, et al. Quantitation of Cremophor EL in human plasma samples using a colorimetric dye-binding microassay. *Anal Biochem.* 1998; 255(2):171–175. [PubMed: 9451500]
28. Gelderblom H, et al. Cremophor EL: the drawbacks and advantages of vehicle selection for drug formulation. *Eur J Cancer.* 2001; 37(13):1590–1598. [PubMed: 11527683]
29. Kiss L, et al. Kinetic analysis of the toxicity of pharmaceutical excipients Cremophor EL and RH40 on endothelial and epithelial cells. *J Pharm Sci.* 2013; 102(4):1173–1181. [PubMed: 23362123]
30. Huang YY, et al. Stable synthetic bacteriochlorins for photodynamic therapy: role of dicyano peripheral groups, central metal substitution (2H, Zn, Pd), and Cremophor EL delivery. *Chem Med Chem.* 2012; 7(12):2155–2167. [PubMed: 23065820]
31. Sharma SK, et al. Synthesis and evaluation of cationic bacteriochlorin amphiphiles with effective in vitro photodynamic activity against cancer cells at low nanomolar concentration. *J Porphyr Phthalocyanines.* 2013; 17(01–02):73–85. [PubMed: 23956614]
32. Nitzan Y, et al. Structure-activity relationship of porphines for photoinactivation of bacteria. *Photochem Photobiol.* 1995; 62(2):342–347. [PubMed: 7480142]
33. Rajaputra P, et al. Synthesis and in vitro biological evaluation of lipophilic cation conjugated photosensitizers for targeting mitochondria. *Bioorg Med Chem.* 2013; 21(2):379–387. [PubMed: 23245573]
34. Noodt BB, et al. Different apoptotic pathways are induced from various intracellular sites by tetraphenylporphyrins and light. *Br J Cancer.* 1999; 79(1):72–81. [PubMed: 10408696]
35. Chan WS, et al. Photocytotoxic efficacy of sulphonated species of aluminium phthalocyanine against cell monolayers, multicellular spheroids and in vivo tumours. *Br J Cancer.* 1991; 64(5): 827–832. [PubMed: 1931602]
36. Paquette B, et al. Biological activities of phthalocyanines--VIII. Cellular distribution in V-79 Chinese hamster cells and phototoxicity of selectively sulfonated aluminum phthalocyanines. *Photochem Photobiol.* 1988; 47(2):215–220. [PubMed: 3344290]
37. Paquette B, et al. Biological activities of phthalocyanines--XI. Phototoxicity of sulfonated aluminum naphthalocyanines towards V-79 Chinese hamster cells. *Photochem Photobiol.* 1990; 51(3):313–317. [PubMed: 2356226]
38. Selbo PK, et al. Photochemical internalization provides time- and space-controlled endolysosomal escape of therapeutic molecules. *J Control Release.* 2010; 148(1):2–12. [PubMed: 20600406]
39. Martinez de Pinillos Bayona A, et al. Enhancing the efficacy of cytotoxic agents for cancer therapy using photochemical internalisation. *Int J Cancer.* 2016; 138(5):1049–1057. [PubMed: 25758607]
40. Huang YY, Luo D, R HM. Stable Synthetic Bacteriochlorins: Potent Light-Activated Anti-Cancer Drugs. *Curr Org Chem.* 2015; 19(10):948–957.
41. Sharma SK, et al. Synthesis and evaluation of cationic bacteriochlorin amphiphiles with effective photodynamic activity against cancer cells at low nanomolar concentration. *J Porphyr Phthalocyanines.* 2013; 17(1–2):73–85. [PubMed: 23956614]
42. Huang L, et al. Stable synthetic cationic bacteriochlorins as selective antimicrobial photosensitizers. *Antimicrob Agents Chemother.* 2010; 54(9):3834–3841. [PubMed: 20625146]
43. Dror SB, et al. The localization and photosensitization of modified chlorin photosensitizers in artificial membranes. *Photochem Photobiol Sci.* 2009; 8(3):354–361. [PubMed: 19255676]
44. Dougherty TJ, et al. Photodynamic therapy. *J Natl Cancer Inst.* 1998; 90(12):889–905. [PubMed: 9637138]
45. Engbrecht BW, et al. Photofrin-mediated photodynamic therapy induces vascular occlusion and apoptosis in a human sarcoma xenograft model. *Cancer Res.* 1999; 59(17):4334–4342. [PubMed: 10485481]
46. Glanzmann TM, et al. Assessment of a sheep animal model to optimise photodynamic therapy in the oesophagus. *Lasers Surg Med.* 2009; 41(9):643–652. [PubMed: 19790242]
47. Wang LX, et al. Antitumor activity of photodynamic therapy with a chlorin derivative in vitro and in vivo. *Tumour Biol.* 2015
48. Hill RA, et al. Photodynamic therapy of the ciliary body with tin ethyl etiopurpurin and tin octaethyl benzochlorin in pigmented rabbits. *Ophthalmic Surg Lasers.* 1997; 28(11):948–953. [PubMed: 9387183]

49. Garbo GM, et al. Effects of ursodeoxycholic acid on photodynamic therapy in a murine tumor model. *Photochem Photobiol.* 2003; 78(4):407–410. [PubMed: 14626670]
50. Kessel D, Garbo GM, Hampton J. The role of lipoproteins in the distribution of tin etiopurpurin (SnET2) in the tumor-bearing rat. *Photochem Photobiol.* 1993; 57(2):298–301. [PubMed: 8451293]
51. Egorin MJ, et al. Plasma pharmacokinetics and tissue distribution in CD2F1 mice of Pc4 (NSC 676418), a silicone phthalocyanine photodynamic sensitizing agent. *Cancer Chemother Pharmacol.* 1999; 44(4):283–294. [PubMed: 10447575]
52. Melo C, et al. Pharmacokinetics of Photogem using fluorescence monitoring in Wistar rats. *J Photochem Photobiol B.* 2004; 73(3):183–188.
53. Houle JM, Strong A. Clinical pharmacokinetics of verteporfin. *J Clin Pharmacol.* 2002; 42(5):547–557. [PubMed: 12017349]
54. Mori K, et al. Photodynamic therapy of experimental choroidal neovascularization with a hydrophilic photosensitizer: mono-L-aspartyl chlorin e6. *Retina.* 2001; 21(5):499–508. [PubMed: 11642380]
55. Kessel D, Whitcomb KL, Schulz V. Lipoprotein-mediated distribution of N-aspartyl chlorin-E6 in the mouse. *Photochem Photobiol.* 1992; 56(1):51–56. [PubMed: 1508982]
56. Synytsya A, et al. Biodistribution Assessment of a Lutetium (III) Texaphyrin Analogue in Tumor-bearing Mice Using NIR Fourier-transform Raman Spectroscopy. *Photochem Photobiol.* 2004; 79(5):453–460.
57. Peng Q, et al. Sensitizer for photodynamic therapy of cancer: a comparison of the tissue distribution of Photofrin II and aluminum phthalocyanine tetrasulfonate in nude mice bearing a human malignant tumor. *Int J Cancer.* 1991; 48(2):258–264. [PubMed: 1826901]
58. Lepor H. Vascular targeted photodynamic therapy for localized prostate cancer. *Rev Urol.* 2008; 10(4):254–261. [PubMed: 19145269]
59. Mazor O, et al. WST11, a novel water-soluble bacteriochlorophyll derivative; cellular uptake, pharmacokinetics, biodistribution and vascular-targeted photodynamic activity using melanoma tumors as a model. *Photochem Photobiol.* 2005; 81(2):342–351. [PubMed: 15623318]
60. Brun PH, et al. Determination of the in vivo pharmacokinetics of palladium-bacteriopheophorbide (WST09) in EMT6 tumour-bearing Balb/c mice using graphite furnace atomic absorption spectroscopy. *Photochem Photobiol Sci.* 2004; 3(11–12):1006–1010.
61. Ocakoglu K, et al. (131)I-Zn-Chlorophyll derivative photosensitizer for tumor imaging and photodynamic therapy. *Int J Pharm.* 2015; 493(1–2):96–101. [PubMed: 26226337]
62. Ocakoglu K, et al. Evaluation of cancer imaging potential and photodynamic therapy efficacy of copper (II) benzylxyphorbide-a. *J Drug Target.* 2015; 23(1):89–95. [PubMed: 25230852]
63. Paul B, Rajaputra P, You Y. In vitro and in vivo photodynamic activity of core-modified porphyrin IY69 using 690 nm diode laser. *Photochem Photobiol.* 2011; 87(6):1468–1473. [PubMed: 21854396]
64. Mitra S, Mironov O, Foster TH. Confocal fluorescence imaging enables noninvasive quantitative assessment of host cell populations in vivo following photodynamic therapy. *Theranostics.* 2012; 2(9):840–849. [PubMed: 23082097]
65. Zheng X, et al. Conjugation of 2-(1'-Hexyloxyethyl)-2-devinylpyropheophorbide-a (HPPH) to Carbohydrates Changes its Subcellular Distribution and Enhances Photodynamic Activity in Vivo. *J Med Chem.* 2009; 52(14):4306–4318. [PubMed: 19507863]
66. Wang X, et al. Analysis of the in vivo and in vitro effects of photodynamic therapy on breast cancer by using a sensitizer, sinoporphyrin sodium. *Theranostics.* 2015; 5(7):772–786. [PubMed: 25897341]
67. Yakubovskaya RI, et al. Photophysical properties and in vitro and in vivo photoinduced antitumor activity of cationic salts of meso-tetrakis(N-alkyl-3-pyridyl)bacteriochlorins. *J Photochem Photobiol B.* 2014; 130:109–114. [PubMed: 24316046]
68. Biswas R, Moon JH, Ahn JC. Chlorin e6 derivative radachlorin mainly accumulates in mitochondria, lysosome and endoplasmic reticulum and shows high affinity toward tumors in nude mice in photodynamic therapy. *Photochem Photobiol.* 2014; 90(5):1108–1118. [PubMed: 24666230]



69. Yslas EI, et al. Biodistribution and phototherapeutic properties of Zinc (II) 2,9,16,23-tetrakis (methoxy) phthalocyanine in vivo. *Photodiagnosis Photodyn Ther.* 2009; 6(1):62–70. [PubMed: 19447373]
70. Shemesh CS, Moshkelani D, Zhang H. Thermosensitive liposome formulated indocyanine green for near-infrared triggered photodynamic therapy: in vivo evaluation for triple-negative breast cancer. *Pharm Res.* 2015; 32(5):1604–1614. [PubMed: 25407543]
71. Lassalle HP, et al. Correlation between in vivo pharmacokinetics, intratumoral distribution and photodynamic efficiency of liposomal mTHPC. *J Control Release.* 2009; 134(2):118–124. [PubMed: 19100297]
72. Jones HJ, Vernon DI, Brown SB. Photodynamic therapy effect of m-THPC (Foscan) in vivo: correlation with pharmacokinetics. *Br J Cancer.* 2003; 89(2):398–404. [PubMed: 12865935]
73. Bovis MJ, et al. Improved in vivo delivery of m-THPC via pegylated liposomes for use in photodynamic therapy. *J Control Release.* 2012; 157(2):196–205. [PubMed: 21982898]
74. Rapozzi V, et al. Conjugated PDT drug: photosensitizing activity and tissue distribution of PEGylated pheophorbide a. *Cancer Biol Ther.* 2010; 10(5):471–482. [PubMed: 20592494]
75. Rapozzi V, et al. The PDT activity of free and pegylated pheophorbide a against an amelanotic melanoma transplanted in C57/BL6 mice. *Invest New Drugs.* 2013; 31(1):192–199. [PubMed: 22688292]

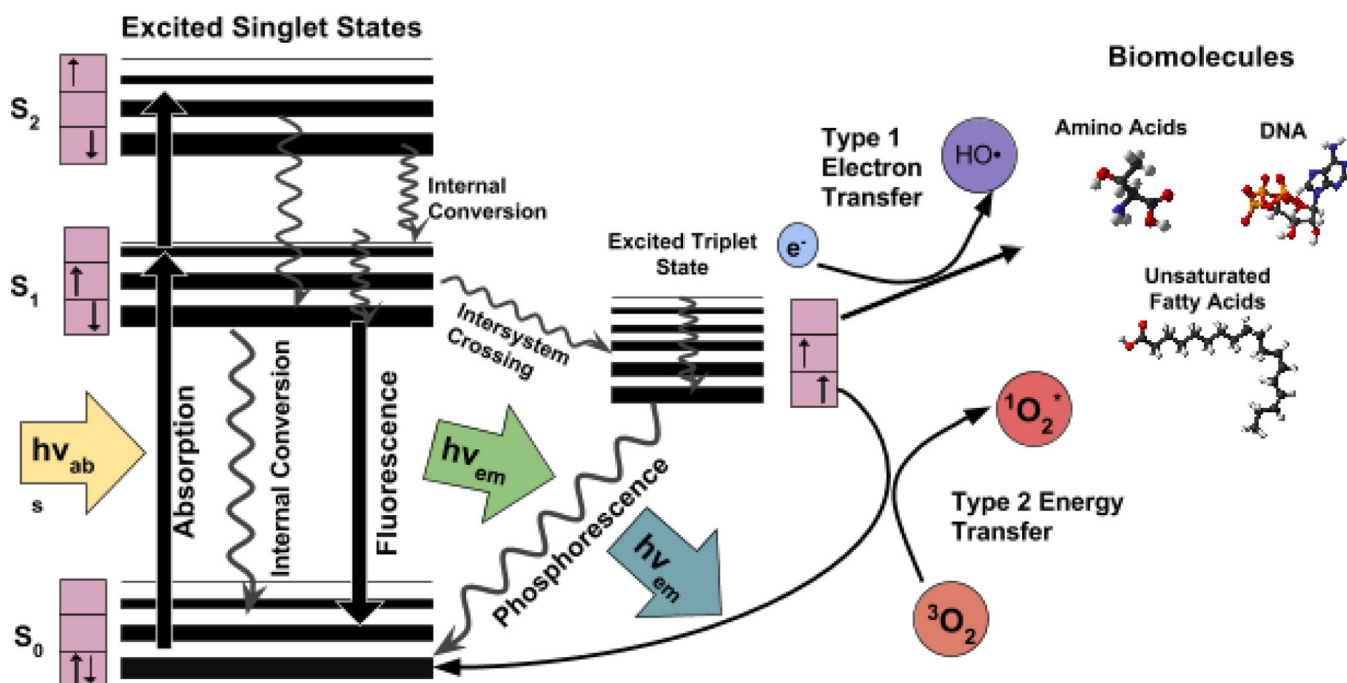


**Figure 1.** Jablonski diagram illustrating the different electronic energy levels and transitions between them after photon excitation.

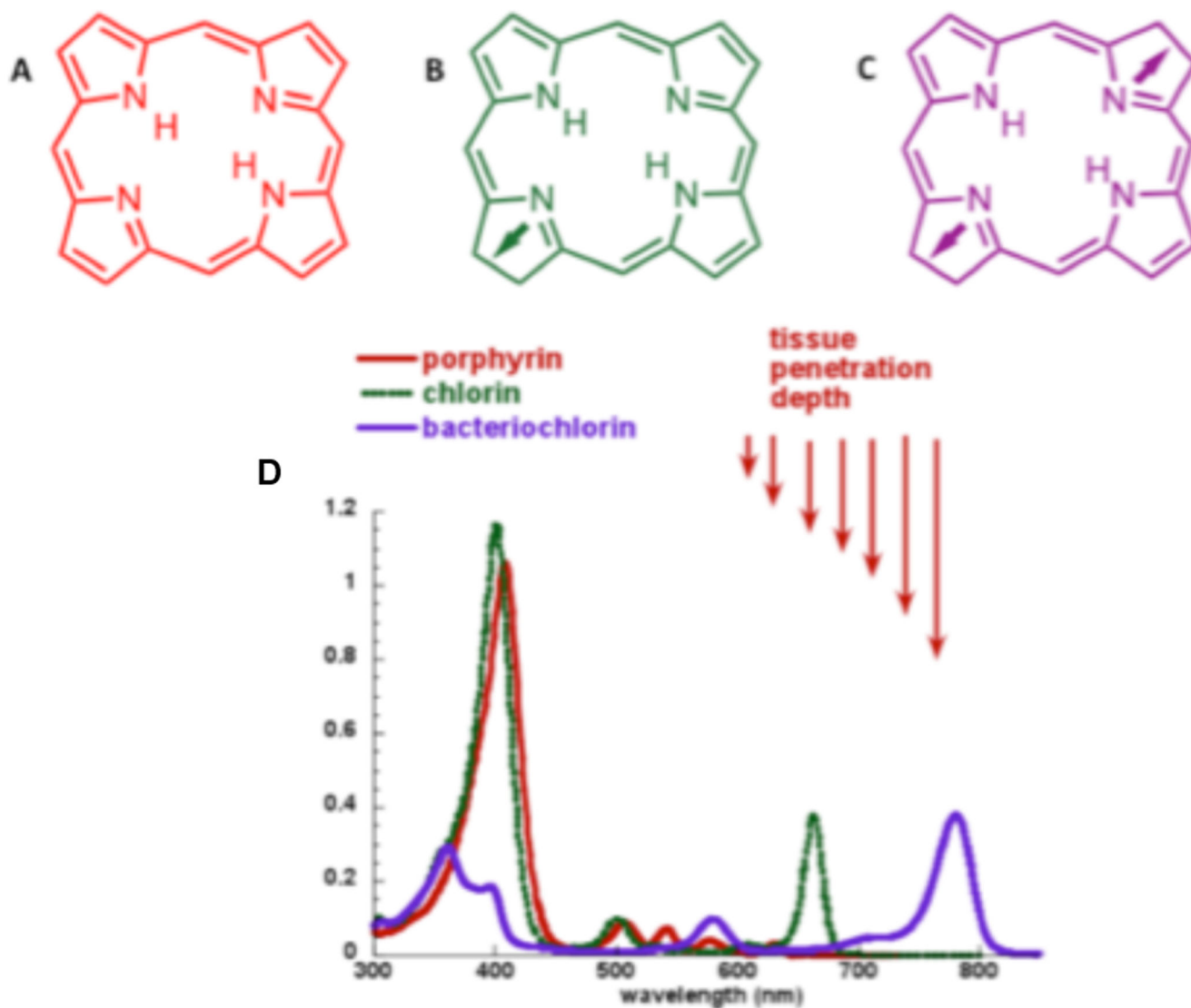


**Figure 2.** Backbone chemical structures and absorption spectra of tetrapyrrole photosensitizers A) porphyrin, B) chlorin, C) bacteriochlorin, D) absorption spectra.

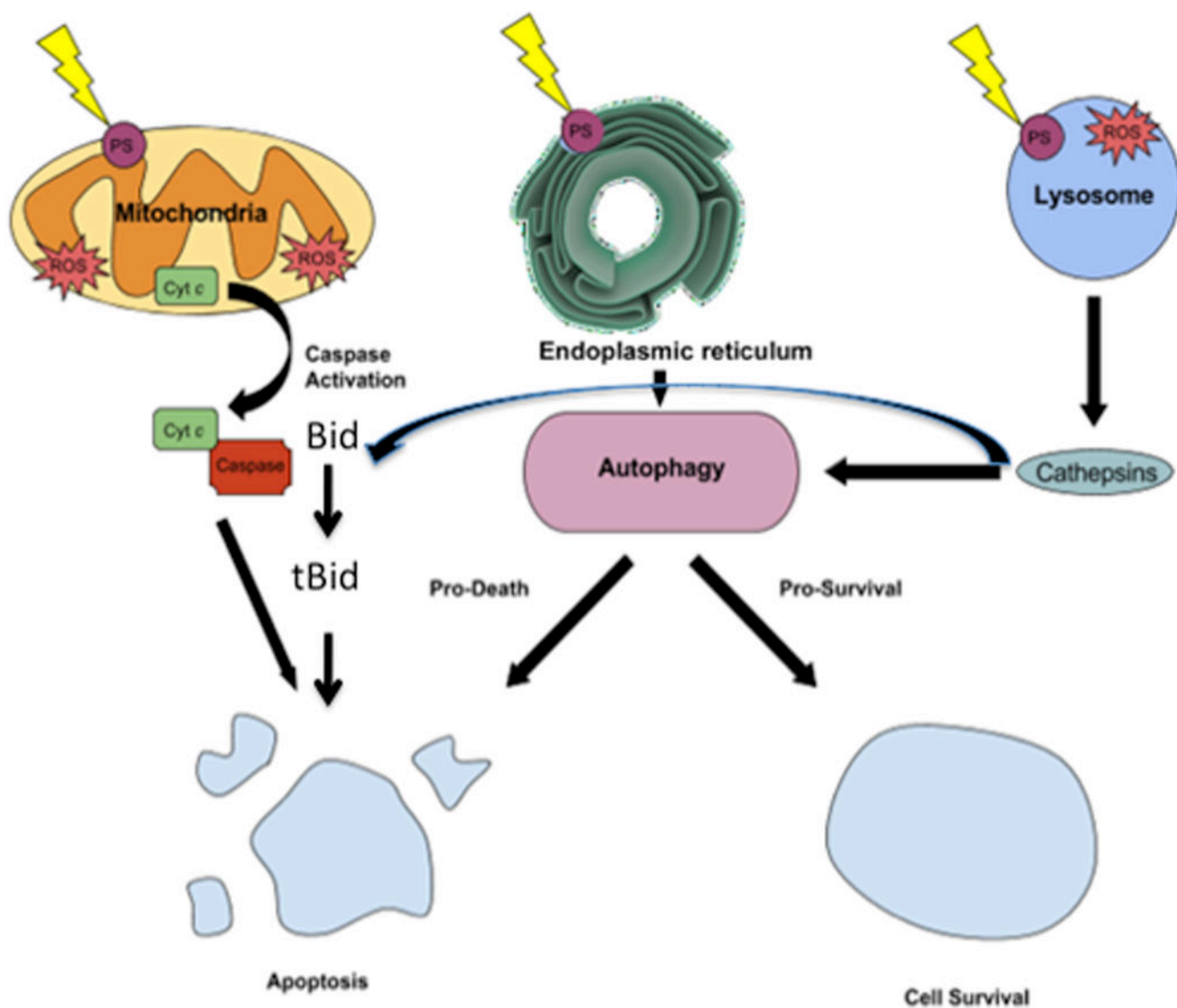
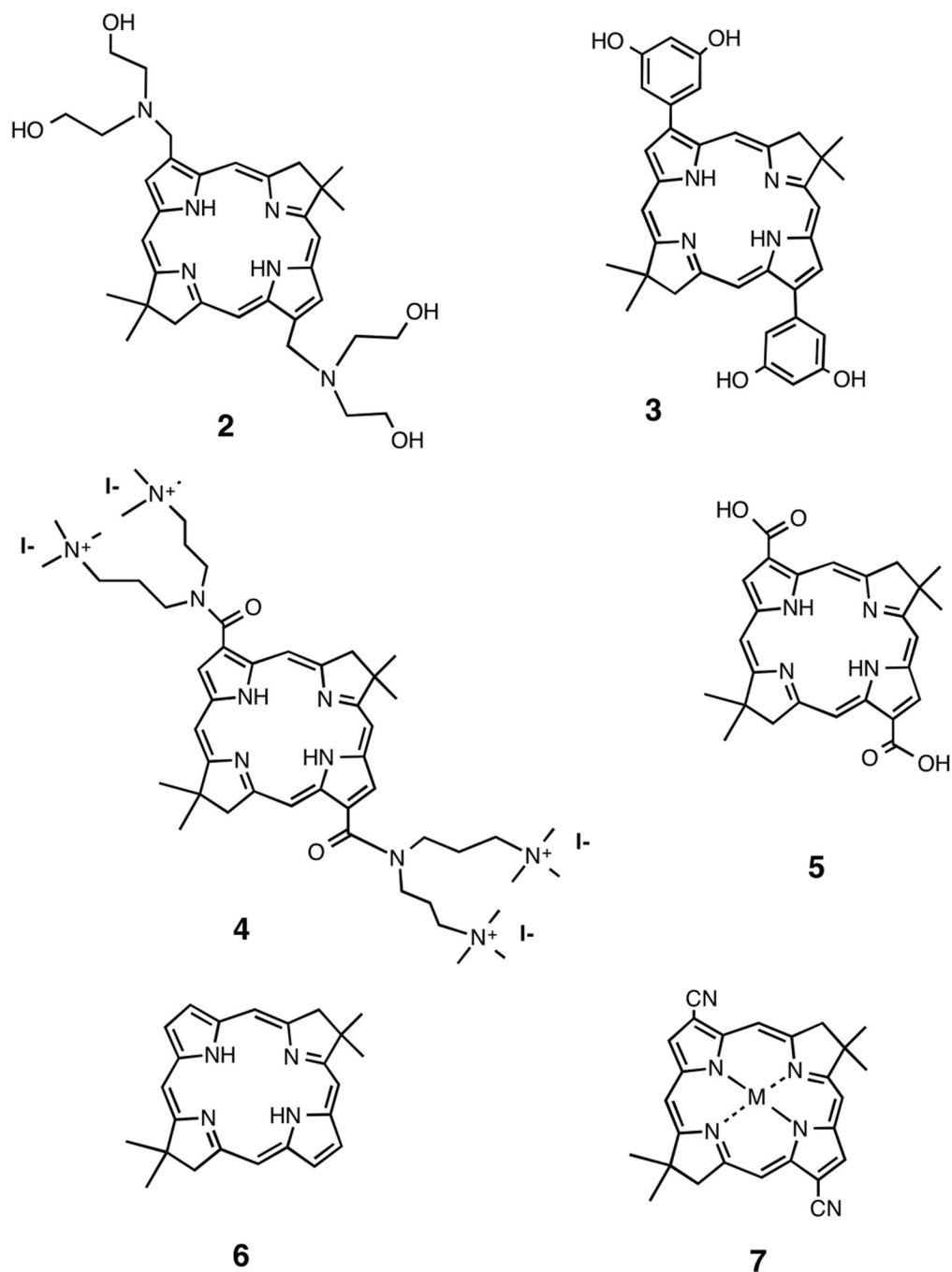
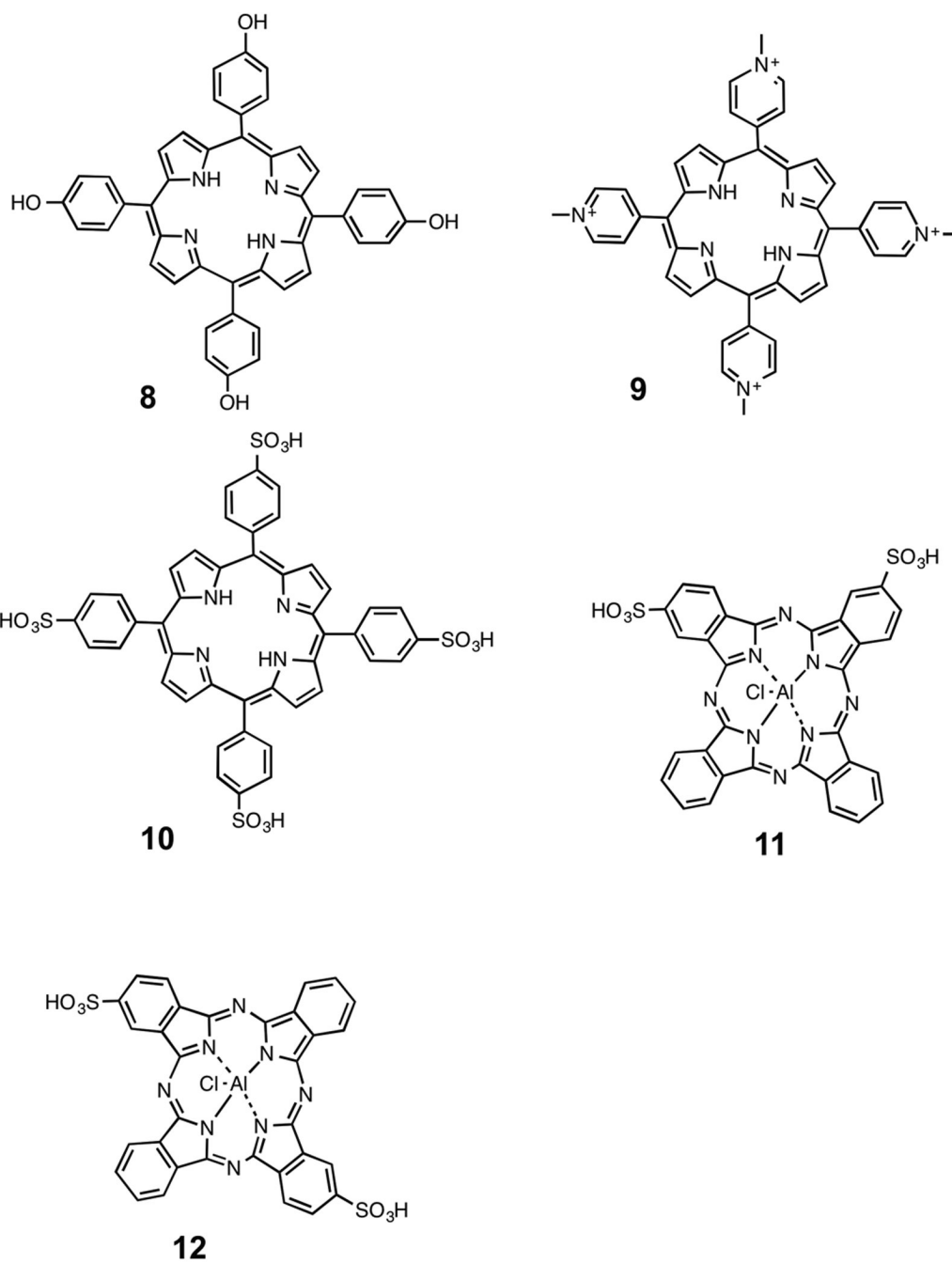


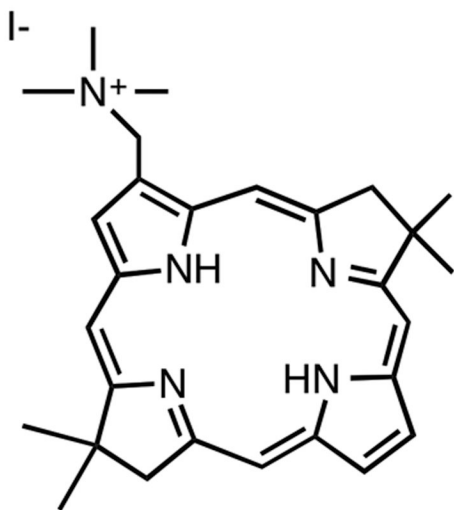
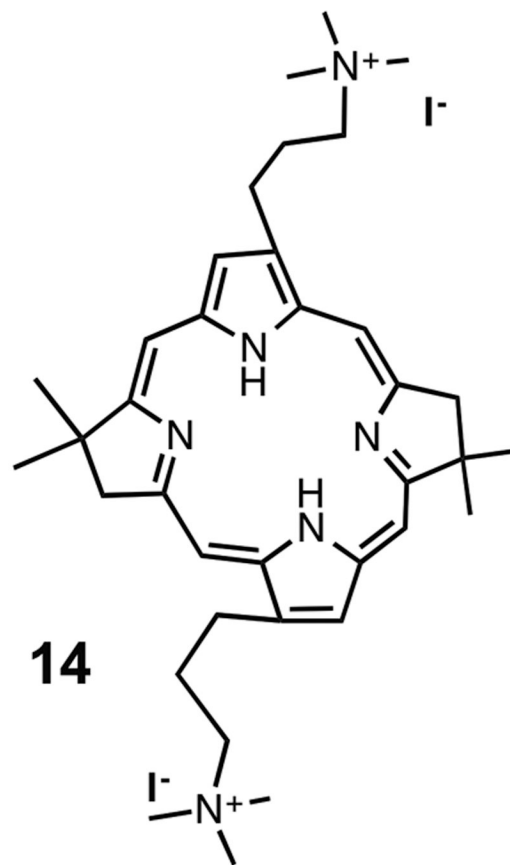
**Figure 3.** Cell death mechanisms illustrating some of the main death pathways. PS localized in mitochondria lead to apoptosis via release of cytochrome c and activation of caspase 3; PS localized in endoplasmic reticulum cause ER-stress leading to autophagy that can result in death or survival; PS localized in lysosomes can lead to release of cathepsins that can also cause apoptosis.



scheme 1.

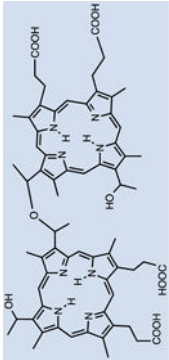
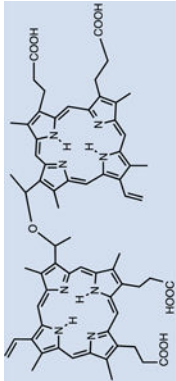
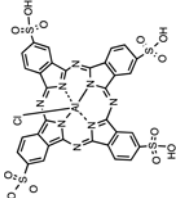
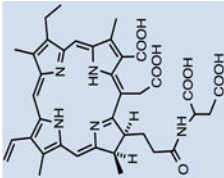


scheme 2.

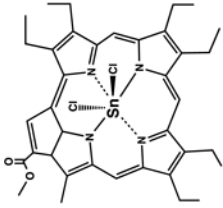
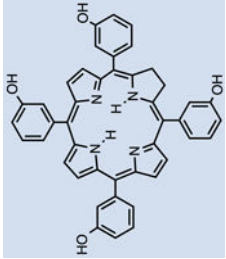
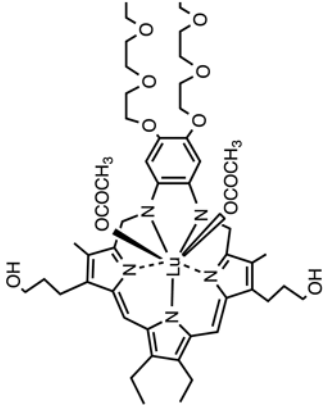
**13****14**

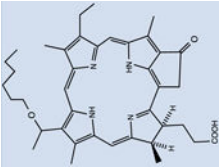
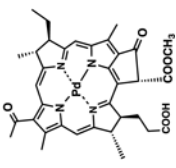
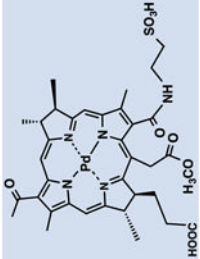
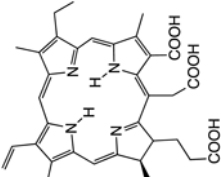
scheme 3.

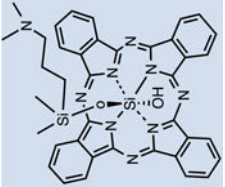
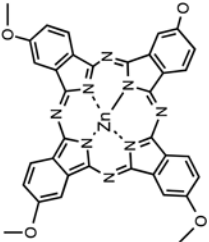
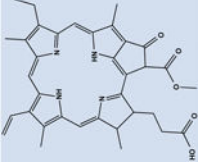
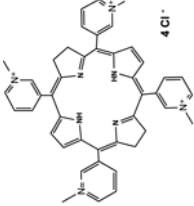
Table 1

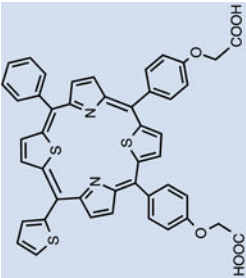
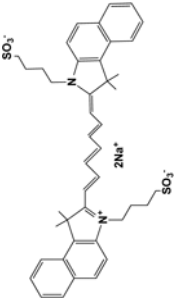
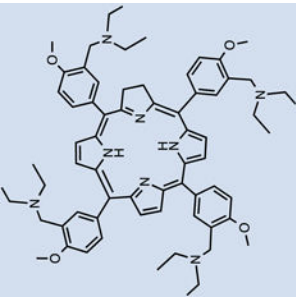
Photosensitizer	N°	Structure	Delivery vehicle	Injection site	Dose (mg/kg)	Maximal tumor uptake (hr post injection)	Ref.
Photofrin	1		Aqueous solution	I.P.	20	12-72	[56]
Photogem®	15		-	I.V.	1.5	-	[51]
Sinoporphyrin sodium (DVDMS)	16		Saline solution	I.V.	2	12	[65]
AIPcS <sub>4</sub>	17		PBS	I.P.	20	0.5	[56]
NPe6	18		Aqueous solution	I.V.	5	-	[53]



Photosensitizer	N°	Structure	Delivery vehicle	Injection site	Dose (mg/kg)	Maximal tumor uptake (hr post injection)	Ref.
SnET2	19		Lipid emulsion	I.V.	1	-	[47]
Foscan® meta-(tetra-hydroxyphenyl) chlorin m(THPC)	20		H <sub>2</sub> O, polyethylene glycol 400, ethanol (5:3:2 vol/vol/vol) solution	I.V.	0.15	-	[45]
Foslip® (liposomal mTHPC)	21		Aqueous solution	I.V.	0.3	72	[70]
PEG- and non PEG-liposomal mTHPC	22		10mM histidine buffer, 5% glucose	I.V.	0.3	6	[72]
Lutex (LuT <sub>2</sub> B <sub>2</sub> Tex)	23		Aqueous solution	S.C.	60	72	[55]

Photosensitizer	N°	Structure	Delivery vehicle	Injection site	Dose (mg/kg)	Maximal tumor uptake (hr post injection)	Ref.
HPPH, Photochlor	24		-	I.V.	0.33	48	[64]
WST09 (TOOKAD®)	25		alcohol/Cremophor EL® /NaOH	I.V.	5.0 ± 1.0	-	[59]
WST11 (TOOKAD® soluble)	26		PBS	IV.	6	-	[58]
Radachlorin® (Chlorin e6 derivative)	27		Aqueous solution	I.V.	10	6	[67]

Photosensitizer	N°	Structure	Delivery vehicle	Injection site	Dose (mg/kg)	Maximal tumor uptake (hr post injection)	Ref.
Pc4	28		1:2:0.154 M NaCl (1:3, v:v) or polyethylene glycol:Tween 80:sodium phosphate buffer	I.V.	40, 10, 2	-	[50]
Liposomal ZnPc(OCH <sub>2</sub> ) <sub>4</sub> [Zn(II) 2,9,16,23-tetrakis (methoxy) phthalocyanine]	29		Saline solution	I.P. & I.V.	0.2	24 I.V.; 72 I.P. Higher uptake I.V.	[68]
mPEG- Pheophorbide A	30		Saline-DMSO (9 + 1 v/v) or saline solution	I.P.	0.05	-	[73]
Cationic salts of meso-tetrakis (N-alkyl-3-pyridyl) bacteriochlorins	31		NaCl 0.9% aqueous solution	I.V.	2.5-5.0	0.25-0.5min (different for each PS salt)	[66]

Photosensitizer	N°	Structure	Delivery vehicle	Injection site	Dose (mg/kg)	Maximal tumor uptake (hr post injection)	Ref.
IY69 [(5-phenyl)-10,15-bis(4-carboxylatomethoxyphenyl)-20-(2-thienyl)-21,23-dithiaporphyrin]	32		1% Tween 80/5% dextrose solution	I.P.	20	72	[62]
Liposomal indocyanine green (LpICG)	33		-	I.V.	5	4	[69]
meso-tetra[3-(N,N-diethyl)aminomethyl]-4-methoxy]phenyl chlorin (TMPC)	34		-	I.V.	20 mg/kg	1 hr	[46]